Eur. Phys. J. A **21**, 469–478 (2004)
DOI 10.1140/epja/i2004-10005-1

THE EUROPEAN PHYSICAL JOURNAL A

Exclusive photoproduction of charmed D^* vector mesons, $\gamma + N \rightarrow Y_c + \overline{D}^*$, $Y_c = \Lambda_c^+$ or Σ_c

E. Tomasi-Gustafsson[1,a] and M.P. Rekalo[2]

[1] DAPNIA/SPhN, CEA/Saclay, 91191 Gif-sur-Yvette Cedex, France
[2] NSC Kharkov Institute of Physics and Technology, 61108 Kharkov, Ukraine

Received: 11 February 2004 /
Published online: 14 September 2004 –
Communicated by V.V. Anisovich

Abstract. The spin structure of the matrix element for the reactions $\gamma + N \rightarrow Y_c + D^*$, where $Y_c = \Lambda_c^+(2285)$, $\Sigma_c(2455)$ are charmed baryons with spin 1/2, and $D^*(2010)$ is the vector charmed meson, can be parametrized, in collinear regime, in terms of three independent scalar amplitudes, which are functions of the photon energy E_γ, only. In the framework of an effective Lagrangian approach generalized to charm photoproduction, we calculate the energy dependence of the differential cross-section, the density matrix element of $\overline{D}^*$, ρ_{11}, the asymmetry A_z in the collision of circularly polarized photons with polarized nucleons, and the polarization of the produced Y_c-hyperon, P_z, in the collision of circularly polarized photons with unpolarized target. All these polarization observables either vanish or are large, in absolute value, with a smooth E_γ-dependence, and differ for Λ_c^+ and Σ_c production.

PACS. 13.60.-r Photon and charged-lepton interactions with hadrons – 13.88.+e Polarization in interactions and scattering – 14.40.Lb Charmed mesons – 14.20.Lq Charmed baryons

1 Introduction

In a previous paper [1] we analyzed the exclusive processes of charm pseudoscalar meson D^0 photoproduction, $\gamma + N \rightarrow Y_c + \overline{D}$, $Y_c = \Lambda_c^+$, or Σ_c. We consider here the exclusive processes of charmed vector meson D^* photoproduction, $\gamma + N \rightarrow Y_c + \overline{D}^*$, on proton and neutron targets. No detailed theoretical analysis exists for such processes, and up to now, experimentally, only an indirect evaluation of their cross-section has been done. In ref. [2], an attempt has been done to estimate the contribution of the processes $\gamma + N \rightarrow Y_c + \overline{D}(\overline{D}^*)$ to the asymmetry of the collisions of a circularly polarized photon beam with a polarized target in $\boldsymbol{\gamma} + \mathbf{N} \rightarrow$ open charm $+X$. It is well known that such asymmetry is sensitive to the ΔG gluon contribution to the nucleon spin [3]. In ref. [4] the D-exchange contribution has been calculated for $\gamma + N \rightarrow Y_c + \overline{D}^*$, in the near-threshold region, considering the possible baryon exchange as a background process.

Let us list some arguments to justify the interest in exclusive charmed vector meson photoproduction:

– their contribution to the total cross-section is important, especially in the near-threshold region;
– the understanding of the reaction mechanisms requires the deconvolution of these channels;
– these reactions naturally explain the particle-antiparticle asymmetry in charmed particles photoproduction, at high energies;
– the polarization phenomena induced by the production of vector mesons are new, interesting and measurable (the D^*-meson is a self-analyzing particle, through the angular dependence of the decay products in $D^* \rightarrow D + \pi$, but this decay does not allow to access the vector D^*-meson polarization);
– direct experimental data, concerning these reactions, are expected soon, due to the higher luminosity of ongoing experiments, as COMPASS [5].

There are essential differences between the processes of exclusive photoproduction of light vector mesons (ρ, ω, ϕ or K^*) and heavy D^* production. In the last case, the diffractive mechanism is absent and the large mass of the c-quark seems to justify the applicability of perturbative QCD. However, there is no direct relation between the photon-gluon fusion subprocess, $\gamma + G \rightarrow c + \overline{c}$ and the exclusive D^* photoproduction. Therefore, QCD-inspired models, like the effective Lagrangian approach (ELA), in terms of hadronic degrees of freedom, as charmed baryons and mesons, seem more appropriate. In such approach, it is possible to predict the differential cross-section and all

[a] e-mail: etomasi@cea.fr

polarization observables in terms of a finite number of coupling constants, of strong and electromagnetic nature —in any kinematical condition. The same coupling constants enter also in the calculation of other processes of associative charm production in πN, γN and NN collisons.

There are experimental data about inclusive D^* photoproduction, $\gamma + p \to D^* + X$ or $e^- + N \to e^- + D^* + X$ up to HERA energies [6]. The smallest energy, where D^* photoproduction has been observed is $E_\gamma = 20\,\mathrm{GeV}$, at SLAC [7]. Typically, D^* production is the main channel for $\gamma + N \to$ charm $+X$ [6–12], so that the ratio between the vector (V) and the total D^* contribution to the total cross-section is in agreement with the spin quark rule $V/(P+V) \simeq 0.75$, where P is the pseudoscalar contribution. The relative role of the charged and neutral D-meson photoproduction depends, on one side, on the relative cross-sections for the $D^{*\pm}$ and D^{*0} photoproduction, and, on another side, on the branching ratio for the decays $D^* \to D + \pi$ (for different charge combinations).

We consider here the exclusive processes $\gamma + N \to Y_c + \overline{D}^*$, in case of collinear kinematics, where helicity conservation and the P-invariance of electromagnetic interaction allow three amplitudes, only, which are functions of a single kinematical variable, the photon energy E_γ. Note, in this respect, that generally the processes $\gamma + N \to Y_c + \overline{D}^*$ are characterized by a set of twelve independent amplitudes, which are complex functions of two kinematical variables. Therefore, the theoretical analysis is largely simplified in collinear kinematics.

This paper is organized as follows. In sect. 2 the spin structure of the collinear matrix element is given in terms of three amplitudes, which allows to develop a general and model-independent formalism for the analysis of polarization phenomena. The expressions for the different possible pole contributions, in the framework of ELA approach, are derived in sect. 3. The strong and electromagnetic coupling constants as well as the form factors are discussed in sect. 4. Numerical predictions for the differential cross-section, the single- and double-spin polarization observables, as functions of E_γ, are given in sect. 5. Concluding remarks are given in sect. 6. The appendix contains the explicit expressions of the collinear amplitudes.

2 Collinear amplitudes and polarization phenomena

We consider here the processes $\gamma + N \to Y_c + \overline{D}^*$, $Y_c = \Lambda_c^+$, or Σ_c, $\overline{D}^* = \overline{D}^{*0}$ or $\overline{D}^{*-}$, in collinear regime, *i.e.* for $\theta = 0$ or π, where θ is the $\overline{D}^{*-}$ production angle in the reaction CMS. The reasons of this choice are the following:

- the differential cross-section, $\mathrm{d}\sigma/\mathrm{d}t$, as a rule, is maximal in the forward direction (t is the momentum transfer squared);
- the total helicity of the interacting particles is conserved, for any reaction mechanisms, which implies that the spin structure of the matrix element and the polarization phenomena are highly simplified.

At high photon energies, collinear kinematics is very near to the condition of forward detection of the running experiments, such as COMPASS [5].

Taking into account the P-invariance of the electromagnetic interaction of charmed particles and the helicity conservation, one can write the following general parametrization of the matrix element for any process $\gamma + N \to Y_c + \overline{D}^*$, in collinear kinematics (which holds for any reaction mechanism):

$$\mathcal{M}\big(\gamma N \to Y_c \overline{D}^*\big) = \chi_2^\dagger \Big[\boldsymbol{\epsilon} \cdot \mathbf{U}^* f_1 + i\boldsymbol{\sigma} \cdot \hat{\mathbf{k}}\boldsymbol{\epsilon} \times \hat{\mathbf{k}} \cdot \mathbf{U}^* f_2 + i\boldsymbol{\sigma} \cdot \boldsymbol{\epsilon} \times \hat{\mathbf{k}}\mathbf{U}^* \cdot \hat{\mathbf{k}} f_3\Big] \chi_1 , \qquad (1)$$

with the following notations:

- χ_1 and χ_2 are the two-component spinors of the initial nucleon and the produced Y_c-hyperon,
- $\boldsymbol{\epsilon}$ and $\mathbf{U}$ are the three-vector of the photon and of the $\overline{D}^*$-meson polarizations, with the condition $\boldsymbol{\epsilon} \cdot \hat{\mathbf{k}} = 0$,
- $\hat{\mathbf{k}}$ is the unit vector along the three-momentum of γ;
- f_i, $i = 1$–3, are the collinear amplitudes, which are generally complex functions of a single variable, E_γ.

Using this parametrization, one can find for the differential cross-section:

$$\frac{\mathrm{d}\sigma}{\mathrm{d}t} = \mathcal{N}\left[|f_1|^2 + |f_2|^2 + \frac{E_v^2}{m_v^2}|f_3|^2\right], \qquad (2)$$

where $\mathcal{N}$ is a normalization factor, E_v (m_v) is the energy (mass) of the produced vector meson:

$$E_v = \frac{s + m_v^2 - M^2}{2W}, \quad s = W^2 = m^2 + 2mE_\gamma , \qquad (3)$$

where m (M) is the nucleon (Y_c-hyperon) mass, E_γ is the photon energy in the laboratory (Lab) system.

The D^*-mesons, produced in collinear kinematics, are generally polarized, (with tensor polarization) even in collisions of unpolarized particles:

$$\mathcal{D}\rho_{11} = \frac{|f_1|^2 + |f_2|^2}{2}, \quad \mathcal{D} = |f_1|^2 + |f_2|^2 + \frac{E_v^2}{m_v^2}|f_3|^2 \qquad (4)$$

with the normalization condition: $2\rho_{11} + \rho_{00} = 1$. The non-diagonal elements for ρ_{ab} are equal to zero, in collinear regime.

All the other single-spin polarization observables, such as the Σ_B-asymmetry (with linearly polarized photons interacting with unpolarized target), the analyzing power A (induced by polarized nucleon target) and the final Y_c polarization (in the collision of unpolarized particles), vanish for the considered reactions, for any photon energy and for any reaction mechanism, due to the axial symmetry of collinear kinematics. However, an interesting set of double-spin polarization observables can be measured, for the reactions $\gamma + N \to Y_c + \overline{D}^*$:

- *The asymmetry* A_z in the collision of circularly polarized photon beam, with a polarized nucleon target, in the $\hat{\mathbf{k}}$-direction, which we choose as the z-direction,

$$A_z \mathcal{D} = -2\,\mathrm{Re}\ f_1 f_2^* - |f_3|^2 \frac{E_v^2}{m_v^2} . \qquad (5)$$

Due to the P-invariance of the electromagnetic interaction, the asymmetry for a linearly polarized photon beam vanish, even in collisions with polarized target. In the same way, the linear photon polarization cannot induce any polarization of the emitted Y_c-hyperon (for simplicity, we will assume here 100% photon polarization, with helicity $\lambda_\gamma = +1$).

– In the collision of circularly polarized photons with unpolarized target, the Y_c-hyperon can be longitudinally polarized, and *the polarization* P_z is

$$P_z\mathcal{D} = -2\,\mathrm{Re}\ f_1 f_2^* + |f_3|^2\frac{E_v^2}{m_v^2}\,. \tag{6}$$

– The non-zero components of *the depolarization tensor*, D_{ab}, describing the dependence of the b-component of the Y_c polarization on the a-component of the target polarization can be written as

$$\begin{aligned} D_{zz}\mathcal{D} &= |f_1|^2 + |f_2|^2 - |f_3|^2\frac{E_v^2}{m_v^2}\,, \\ D_{xx}\mathcal{D} &= D_{yy}\mathcal{D} = |f_1|^2 - |f_2|^2. \end{aligned} \tag{7}$$

One can see that these observables are not independent, and the following relations hold, at any photon energy and for any reaction mechanism:

$$D_{zz} = -1 + 4\rho_{11}\,, \qquad A_z - P_z = -2 + 4\rho_{11}\,. \tag{8}$$

These formulas show which experiments are necessary to determine the moduli of the collinear amplitudes, $|f_i|$:

$$\begin{aligned} |f_1|^2 &= \left(\rho_{11} + \frac{1}{2}D_{xx}\right)\mathcal{D}, \\ |f_2|^2 &= \left(\rho_{11} - \frac{1}{2}D_{xx}\right)\mathcal{D}, \\ |f_3|^2\frac{E_v^2}{m_v^2} &= (1 - 2\rho_{11})\mathcal{D}. \end{aligned} \tag{9}$$

Therefore, the measurements of ρ_{11} and D_{xx}, together with the differential cross-section $\mathrm{d}\sigma/\mathrm{d}t$, can be considered as the first step of the complete experiment for any collinear reaction of vector meson photoproduction on a nucleon, such as, for example:

$$\begin{aligned} &\gamma + N \longrightarrow N + V, \qquad V = \rho, \omega, \phi, \\ &\gamma + N \longrightarrow Y + K^*, \quad\ Y = \Lambda\text{- or } \Sigma\text{-hyperon}, \\ &\gamma + N \longrightarrow Y_c + \overline{D}^*. \end{aligned} \tag{10}$$

Further experiments are necessary to determine the relative phases of the collinear amplitudes f_i. For example, the relation

$$(P_z + A_z)\mathcal{D} = -4\,\mathrm{Re}\, f_1 f_2^* \tag{11}$$

allows to determine the relative phase, $\delta_1 - \delta_2$, of the amplitudes f_1 and f_2, more exactly, $\cos(\delta_1 - \delta_2)$. T-odd polarization observables are more sensitive to the small relative phase, being determined by $\sin(\delta_1 - \delta_2)$. The simplest of these observables, in collinear regime, is the D^* tensor polarization, induced by polarized target. The corresponding density matrix can be parametrized as follows:

$$\begin{aligned} \rho_{ab}(P) = {}& i\rho_1\epsilon_{abc}P_c + i\rho_2\epsilon_{abc}\hat{k}_c\hat{\mathbf{k}}\cdot\mathbf{P} \\ &+\rho_3\left[\hat{k}_a\left(\hat{\mathbf{k}}\times\mathbf{P}\right)_b + \hat{k}_b\left(\hat{\mathbf{k}}\times\mathbf{P}\right)_a\right], \end{aligned} \tag{12}$$

where ρ_i, $i = 1$–3, are real coefficients, quadratic functions of the collinear amplitudes and $\mathbf{P}$ is the pseudovector of the target polarization:

$$\begin{aligned} \rho_1\mathcal{D} &= \mathrm{Re}\, f_1 f_3^*\,, \\ \rho_2\mathcal{D} &= \mathrm{Re}\left(-f_1 f_2^* - f_1 f_3^* + f_2 f_3^*\right), \\ \rho_3\mathcal{D} &= \mathrm{Im}\ (f_1 - f_2) f_3^*\,. \end{aligned} \tag{13}$$

Note, in this connection, that the antisymmetrical part of $\rho_{ab}(P)$, which is characterized by the coefficients ρ_1 and ρ_2, describes D^* production with vector polarization. But this polarization cannot be measured through the main decays of D^*: $D^* \to D + \pi$, $D^* \to D + \gamma$, and $D^* \to D + e^+ + e^-$ [13]. The coefficient ρ_3 characterizes the dependence of the D^* tensor polarization on the target polarization, generating the following angular distribution for the decay products in $D^* \to D + \pi$:

$$W(\theta, \phi) \simeq \sin 2\theta \sin\phi, \tag{14}$$

where θ and ϕ are the polar and azimuthal angles of the π-meson (in D^* rest frame) relative to the polarization plane, which is defined by $\hat{\mathbf{k}}$ and $\mathbf{P}$.

Linear photon polarization can also induce polarized D^*-mesons, with the following non-zero elements of density matrix:

$$\begin{aligned} \rho_{11}^{(1)}\mathcal{D} &= \frac{1}{2}\left(|f_1|^2 + |f_2|^2\right), \\ \rho_{1-1}^{(1)}\mathcal{D} &= \frac{1}{2}\left(|f_1|^2 - |f_2|^2\right), \end{aligned} \tag{15}$$

This represents the complete analysis of all possible double-spin polarization observables, for the reactions $\gamma + N \to Y_c + \overline{D}^*$, in collinear kinematics.

3 The matrix elements

In a previous work [1], we considered the processes of photoproduction of pseudoscalar $\overline{D}$-mesons, in $\gamma + N \to Y + \overline{D}$. In this section we analyze the processes $\gamma + N \to Y_c + \overline{D}^*$, following a similar scheme. These two classes of reactions have common properties with the reactions of associative strange-particles production, $\gamma + N \to Y + K$ and $\gamma + N \to Y + K^*$, where $Y = \Lambda$ and Σ, strange hyperons, even if the masses of the produced particles are very different. All these processes have a non-diffractive nature due to the quantum numbers in t-channel, different from the vacuum. It is often assumed that open charm photoproduction occurs through the mechanism of the photon-gluon fusion, $\gamma + G \to c + \overline{c}$ [3], even in

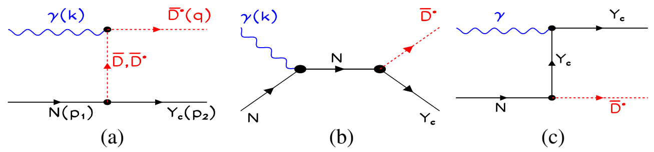

Fig. 1. The pole mechanisms for $\gamma + N \to Y_c + \overline{D^*}$.

the near-threshold region as the applicability of QCD for the considered processes may be justified by the large c-quark mass ($m_c \simeq 1.5\,\mathrm{GeV}$). But, if the elementary process $\gamma + G \to c + \overline{c}$ can be reliably calculated [3], the application to the exclusive processes $\gamma + N \to Y_c + \overline{D}(\overline{D}^*)$ is not straightforward.

The process $\gamma + N \to Y_c + \overline{D}(\overline{D}^*)$ at large photon energy and at small momentum transfer (*i.e.* for forward production), can be analzed as the photoproduction of pseudoscalar (vector) light mesons (π, K) in similar kinematical conditions. In other words, the exclusive processes can be described in terms of non-perturbative models, like any binary processes at large values of the total energy s and of small momentum t, such as Regge-pole description. So, the large mass of c-quarks results in a higher threshold but does not necessarily imply a reaction mechanism of QCD nature. In this framework, the mechanism based on the elementary subprocess $\gamma + G \to c + \overline{c}$ can be viewed as D-meson exchange in t-channel, for the process $\gamma + N \to Y_c + \overline{D}^*$ (fig. 1a). Two other baryon exchanges, the s- and u-contributions, figs. 1b and c, have to be taken into account to insure the gauge invariance of the total matrix element: the conservation of electromagnetic current is a very important property of any photoproduction process.

The matrix element corresponding to these diagrams can be written as follows:

$$\mathcal{M} = \mathcal{M}_t(D) + \mathcal{M}_t(D^*) + \mathcal{M}_s + \mathcal{M}_u\,, \tag{16}$$

where the indices t, s or u indicate the contributions of the corresponding channels.

The exchange by pseudoscalar mesons is described by the following matrix element:

$$\mathcal{M}_t(D) = ie\frac{\kappa(D^*D\gamma)}{m_v(t-m_D^2)}g_{NY_c\overline{D}} \times\overline{u}(p_2)\gamma_5 u(p_1)\epsilon_{\mu\nu\alpha\beta}\epsilon_\mu k_\nu U^*_\alpha q_\beta\,, \tag{17}$$

where $\kappa(D^*D\gamma)$ is the transition magnetic moment describing the electromagnetic decay $D^* \to D + \gamma$, $g_{NY_c\overline{D}}$ is the coupling constant for the vertex $N \to Y_c + \overline{D}$, $\epsilon_\alpha(U_\alpha)$ is the four-vector of the photon (D^*-meson) polarization, m_D is the mass of the pseudoscalar D-meson, $t = (k-q)^2 = (p_1 - p_2)^2$. The notation of the particle four-momenta is indicated in fig. 1a.

The constant $\kappa(D^*D\gamma)$ determines the width of the radiative decay $D^* \to D\gamma$, through the following formula:

$$\Gamma(D^* \to D\gamma) = \alpha\kappa^2(D^*D\gamma)\frac{m_v}{24}\left(1-\frac{m_D^2}{m_v^2}\right)^3, \tag{18}$$

where $\alpha = e^2/(4\pi) = 1/137$. Evidently, the corresponding width does not allow to find the sign of $\kappa(D^*D\gamma)$, which is important for the calculation of possible interference phenomena, for the above-quoted observables. However, the quark model gives indications on this sign, as we will discuss later.

The matrix element $\mathcal{M}_t(D^*)$, corresponding to vector D^*-exchange can be written as

$$\mathcal{M}_t(D^*) = \frac{e}{t-m_D^2}\overline{u}(p_2)\left[\gamma_\alpha g_1 + g_2\frac{\sigma_{\alpha\nu}Q_\nu}{m+M}\right]u(p_1) \times\left(-g_{\alpha\beta}+\frac{Q_\alpha Q_\beta}{m_v^2}\right)\mathcal{J}_\beta\,, \tag{19}$$

$$\mathcal{J}_\beta = -2\epsilon\cdot q U^*_\beta e(\overline{D}^*) + \kappa(\overline{D}^*)\left[\epsilon_\beta k\cdot U^* - \kappa_\beta\epsilon\cdot U^*\right] + (\dots) \tag{20}$$

with the following notations:

- $e(D^*)$ and $\kappa(D^*)$ are the electric charge and the anomalous magnetic moment of the produced $\overline{D}^*$-meson, $e(D^{*0}) = 0$, $e(D^{*-}) = -1$;
- $Q = p_1 - p_2$ is the four-momentum of the virtual D^*-meson (fig. 1a);
- g_1 and g_2 are the vector and tensor coupling constants for the vertex $N \to Y_c + \overline{D}^*$.

The term $(\dots)$ in eq. (20) denotes the possible contribution due to the anomalous quadrupole moment of D^*, which is generally different from zero, even for the neutral D^*-meson due to the charm content of this meson. For the same reason, $\kappa(D^{*0}) \neq 0$. All these electromagnetic constants are not known experimentally, therefore we will neglect in our calculations possible contributions from the D^*-quadrupole moment.

The one-nucleon exchange is described by the following matrix element:

$$\mathcal{M}_s = \frac{e}{s-m^2}\overline{u}(p_2)\left(g_1\hat{U} + g_2\frac{\hat{U}\hat{q}}{m+M}\right) \times\left(\hat{k}+\hat{p}_1+m\right)\left[\hat{\epsilon}e(N) - \frac{\kappa(N)}{2m}\hat{\epsilon}\hat{k}\right]u(p_1), \tag{21}$$

where $s = (k+p_1)^2$, $e(N)$ and $\kappa(N)$ are the electric charge and the anomalous magnetic moment of the target nucleon, $e(n) = 0$, $e(p) = 1$, $\kappa(n) = -1.91$ and $\kappa(p) = 1.79$.

Finally, the matrix element due to the exchange of Y_c-hyperon is

$$\mathcal{M}_u = \frac{e}{u-M^2}\overline{u}(p_2)\left[\hat{\epsilon}e(Y) - \frac{\kappa(Y)}{2M}\hat{\epsilon}\hat{k}\right] \times\left(\hat{p}_2-\hat{k}+M\right)\left(g_1\hat{U} + g_2\frac{\hat{U}\hat{q}}{m+M}\right)u(p_1), \tag{22}$$

where $u = (k-p_2)^2$, $e(Y)$ and $\kappa(Y)$ are the electric charge and the anomalous magnetic moment of the Y_c-hyperon: $e(Y) = +1$ for Λ_c^+ and Σ_c^+, $e(Y) = +2$ for Σ_c^{++} and $e(Y) = 0$ for Σ_c^0. The anomalous magnetic moment $\kappa(Y)$ is experimentally unknown for any charmed hyperon.

Let us briefly discuss the gauge invariance of the suggested model. All contributions induced by the particle magnetic moments, $\kappa(D^*D\gamma)$, $\kappa(D^*)$, $\kappa(N)$, and $\kappa(Y)$ are automatically gauge invariant, independently on the numerical value of these quantities. For the terms of the matrix element, which are induced by the electrical charges of the particles, the corresponding divergency of the electromagnetic current is determined by the following formula:

$$\Delta\mathcal{M}=\mathcal{M}\big(\gamma N\to Y_c\overline{D}^*\big) \stackrel{\epsilon\to k}{=} e\big[e(N)-e\big(\overline{D}^*\big)-e(Y)\big]u(p_2) \times\left(g_1\hat{U}+g_2\frac{\hat{U}\hat{q}}{m+M}\right)u(p_1)+\Delta\mathcal{M}', \quad (23)$$

$$\Delta\mathcal{M}'=\overline{u}(p_2)\left[g_1\frac{m-M}{m_v^2}U\cdot k+g_2\frac{\sigma_{\alpha\beta}U_\alpha k_\beta}{m+M}\right]u(p_1). \quad (24)$$

From the conservation of electric charge in the considered reactions, $e(N)=e(\overline{D}^*)+e(Y)$, it follows that $\Delta\mathcal{M}=\Delta\mathcal{M}'\neq 0$, *i.e.* this part of the matrix element violates the gauge invariance[1].

In conditions of collinear kinematics, however, the situation with gauge invariance is essentially simplified. To show this, let us consider an "improved" matrix element, made gauge invariant by the following substitution:

$$\mathcal{M}\longrightarrow\mathcal{M}'=\mathcal{M}-\frac{\epsilon\cdot\overline{p}}{k\cdot\overline{p}}\Delta\mathcal{M}', \quad (25)$$

where $\overline{p}$ is a four-vector, built generally as a linear combination of the particle four-momenta:

$$\overline{p}=ak+bp_1+cq, \quad (26)$$

where the coefficients a, b, and c are arbitrary functions of the Mandelstam variables s and t. With this transformation the resulting matrix element, $\mathcal{M}'$, is gauge invariant. But in collinear kinematics $\epsilon\cdot\overline{p}=0$, for any choice of a, b, and c, so, when $\boldsymbol{\epsilon}$ is transverse, $\boldsymbol{\epsilon}\cdot\mathbf{k}=0$, we find $\mathcal{M}'=\mathcal{M}$. Therefore, all calculations using this transverse gauge condition, which holds in the reaction CMS, can be done on the basis of eqs. (17), (20), (21), and (22), for different matrix elements, without violating gauge invariance.

Note, in this respect, that the contribution to the amplitudes f_i which is proportional to the D^* electric charge, $e(D^*)$, vanishes in collinear kinematics, see eq. (20).

The explicit expressions for the collinear amplitudes f_i, $i=1,2,3$, corresponding to the different matrix elements, see eqs. (17), (20), (21), and (22), are given in the appendix. In the considered model, these amplitudes are real functions of E_γ.

[1] The g_1-ccontribution to $\Delta\mathcal{M}'$ can be cancelled by the "catastrophic" diagram. The corresponding predictions [14] for the cross-sections of the processes $\gamma+N\to Y_c+\overline{D}(\overline{D}^*)$, in the threshold region, are in contradiction with the experimental data [15].

4 The electromagnetic coupling constants and the form factors

We consider here the six possible binary reactions of D^* photoproduction:

$$\begin{aligned}
&\gamma+p\longrightarrow\Lambda_c^++\overline{D}^{*0}, \quad \gamma+n\longrightarrow\Lambda_c^++D^{*-},\\
&\gamma+p\longrightarrow\Sigma_c^++\overline{D}^{*0}, \quad \gamma+n\longrightarrow\Sigma_c^++D^{*-},\\
&\gamma+p\longrightarrow\Sigma_c^{++}+D^{*-}, \quad \gamma+n\longrightarrow\Sigma_c^0+\overline{D^{*0}},
\end{aligned} \quad (27)$$

and calculate the E_γ-dependence of the following observables: $\mathrm{d}\sigma/\mathrm{d}t$, ρ_{11}, A_z and P_z for each of the reactions (27).

The corresponding collinear amplitudes are linear functions of the strong coupling constants for the two vertices, $N\to Y_c+\overline{D}$ and $N\to Y_c+\overline{D}^*$. So, taking into account the isotopic invariance of the strong interaction, it is necessary to know at least six independent coupling constants:

$$\begin{aligned}
g_{1\Sigma}&\equiv g_1\big(p\Sigma_c^+\overline{D}^{*0}\big),\\
g_{1\Lambda}&\equiv g_1\big(p\Lambda_c^+\overline{D}^{*0}\big),\\
r_{12}(\Sigma)&\equiv g_2\big(p\Sigma_c^+\overline{D}^{*0}\big)/g_1\big(p\Sigma_c^+\overline{D}^{*0}\big),\\
r_{12}(\Lambda)&\equiv g_2\big(p\Lambda_c^+\overline{D}^{*0}\big)/g_1\big(p\Lambda_c^+\overline{D}^{*0}\big),\\
r(\Sigma)&\equiv g\big(p\Sigma_c^+\overline{D}^{0}\big)/g_1\big(p\Sigma_c^+\overline{D}^{*0}\big),\\
r(\Lambda)&\equiv g\big(p\Lambda_c^+\overline{D}^{0}\big)/g_1\big(p\Lambda_c^+\overline{D}^{*0}\big),
\end{aligned}$$

So, the two possible processes of Λ_c^+ photoproduction, $\gamma+N\to\Lambda_c^++\overline{D}^*$, can be described by a set of three coupling constants:

$$g_{1\Lambda}, \qquad r_{12}(\Lambda), \qquad \text{and} \qquad r(\Lambda)$$

and the four possible reactions of Σ_c production, $\gamma+N\to\Sigma_c+\overline{D}^*$, can be described by another set of coupling constants:

$$g_{1\Sigma}, \qquad r_{12}(\Sigma), \qquad \text{and} \qquad r(\Sigma).$$

All polarization observables depend on two ratios only, $r_{12}(Y)$ and $r(Y)$, and are independent on the electric charges of the initial nucleon and the produced charmed particles, due to isotopic invariance. The coupling constant $g_{1\Lambda}(g_{1\Sigma})$ is important for the prediction of the absolute value of the differential cross-section, with the following isotopic relations:

$$\begin{aligned}
&g_1^2\big(p\Lambda_c^+\overline{D}^{*0}\big)=g_1^2(n\Lambda_c^+D^{*-}),\\
&g_1^2\big(p\Sigma_c^{++}D^{*-}\big)=g_1^2\big(n\Sigma_c^0\overline{D}^{*0}\big)=2g_1^2\big(p\Sigma_c^+\overline{D}^{*0}\big)=\\
&\qquad=2g_1^2\big(n\Sigma_c^+\overline{D}^{*-}\big).
\end{aligned} \quad (28)$$

But the electromagnetic properties of the nucleon and the charm particles, which strongly depend on the electric charge of the particles, induce large isotopic effects, *i.e.* a strong dependence on the type of reaction. So, for

Table 1. Magnetic moments and anomalous magnetic moments ($\kappa(Y) = \mu(Y) - e(Y)$) of charmed baryons, in units of μ_N, in the framework of the quark model.

Particle	$\mu(Y)$	$\kappa(Y)$
Λ_c^+	0.42	−0.58
Σ_c^+	0.45	−0.55
Σ_c^{++}	2.33	0.33
Σ_c^0	−1.44	−1.44

the numerical estimations it is necessary to know the following magnetic moments of charmed baryons and $D^* \to D + \gamma$ electromagnetic transitions: $\kappa(Y_c)$, $\kappa(D^{*-}D^{*-}\gamma)$, and $\kappa(D^{*0}D^0\gamma)$.

The quark model gives prescriptions which relate the magnetic moments of the charmed hyperons to the magnetic moments of the charmed quarks, μ_q, $q = u$, d, or c:

$$\begin{aligned}\mu(\Lambda_c^+) &= \mu_c ,\\ \mu(\Sigma_c^{++}) &= (4\mu_u - \mu_c)/3,\\ \mu(\Sigma_c^+) &= (2\mu_u + 2\mu_d - \mu_c)/3,\\ \mu(\Sigma_c^0) &= (4\mu_d - \mu_c)/3.\end{aligned} \tag{29}$$

The magnetic moments of point-like quarks are determined by the electric charge of the quark and its mass, so

$$\mu_q = \frac{Q_q}{2m_q} , \tag{30}$$

where m_q is the "constituent quark" mass. From the analysis of the nucleon and the usual hyperons magnetic moments, one finds [16]:

$$\mu_u = 1.852\ \mu_N, \qquad \mu_d = -0.9722\ \mu_N, \tag{31}$$

where μ_N is the nucleon magneton. Using these values, one has $m_u = 338\,\text{MeV}$, and $m_d = 322\,\text{MeV}$. Therefore, the current value of $m_c = 1.5\,\text{GeV}$ for the charm quark results in $\mu_c = 0.42\ \mu_N$, and in the values of the magnetic moments and anomalous magnetic moments reported in table 1.

For completeness, let us mention that other prescriptions exist for the calculation of $\kappa(Y)$: $SU(4)$ symmetry [17], bag models [18], different versions of quark model [19], dispersion sum rules [20], etc.

In principle, the reactions $\gamma + N \to Y_c + \overline{D}^*$ can be considered a possible source of information on charm hyperon magnetic moments. In the literature, another possibility of measuring the magnetic moment of Λ_c^+, based on the precession in bending crystals has been discussed [21], but this method cannot be applied to the Σ_c-hyperons, which main decay, $\Sigma_c \to \Lambda_c + \pi$ occurs through the strong interaction.

The quark model can also be used for the prediction of the transition magnetic moments (again in terms of quark magnetic moments):

$$\frac{\kappa(D^{*-}D^-\gamma)}{\kappa(D^{*0}\overline{D}\gamma)} = \frac{\mu_c + \mu_d}{\mu_c + \mu_u} \simeq -0.24.$$

Taking the existing experimental data about D^{*0}, $\text{Br}(D^{+0} \to D^+\gamma) = (1.6 \pm 0.4)\%$, and $\Gamma_T(D^{*+}) = (96 \pm 22)\,\text{keV}$ [16], one can find from eq. (18): $|\kappa(D^{*-}\overline{D}\gamma)| \simeq 1$. Moreover, the quark model allows to fix the sign of this magnetic moment, as $\kappa(D^{*-}\overline{D}\gamma) > 0$.

This allow us to fix all the necessary electromagnetic constants, *i.e.* the absolute values of the magnetic moments and their signs. The signs, in particular, are very important in the analysis of the isotopic effects for these reactions, which are large, in the present model, near threshold, due to the strong interference of the different contributions.

Finally, to fix the strong coupling constants, we use, as in ref. [1], the existing information on the corresponding coupling constants for strange particles, which can be determined from the analysis of the data on photo- and electroproduction of Λ- and Σ-hyperons on protons. We will take the following values [22]:

$$\begin{aligned} g_1(N\Lambda K^*) &= -23.0, & r_{12}(\Lambda) &= 2.5,\\ g_1(N\Sigma^0 K^*) &= -25.0, & r_{12}(\Sigma) &= -1.0,\\ g^2_{K\Lambda N}/4\pi &= 10.6, & g^2_{K\Sigma N}/4\pi &= 1.6,\end{aligned} \tag{32}$$

with $g_{K\Lambda N} < 0$ and $g_{K\Sigma N} > 0$ in agreement with $SU(3)$ constrains. The same holds also for K^*-coupling constants. Using $SU(4)$ symmetry, *i.e.* the substitution $s \to c$, one can find from (32) the necessary coupling constants, for charm particles.

The last problem of the model to be discussed is the parametrization of the phenomenological form factors, which are important ingredients of ELA approaches and are usually introduced for the pole contributions [23, 24]. At each vertex, for D- and D^*-exchanges, one can parametrize the form factor as

$$F_{1,2}(t) = \frac{\Lambda^2_{1,2} - m_D^2}{\Lambda^2_{1,2} - t} , \qquad F_{1,2}(t = m_D^2) = 1, \tag{33}$$

where the index 1(2) corresponds to the electromagnetic (strong) vertex and $\Lambda_{1,2}$ is the corresponding cut-off parameter. The baryon contributions, eqs. (21) and (22), have to be modified by the following form factors:

$$\begin{aligned} F_N(s) &= \frac{\Lambda_N^4}{\Lambda_N^4 + (s - m^2)^2} , \quad \text{for } s\text{-channel},\\ F_Y(u) &= \frac{\Lambda_Y^4}{\Lambda_Y^4 + (u - m^2)^2} , \quad \text{for } u\text{-channel},\end{aligned} \tag{34}$$

where Λ_N and Λ_Y are the corresponding cut-off parameters, generally different from $\Lambda_{1,2}$.

Let us note that the introduction of these form factors violates the gauge invariance of that part of the matrix element, $\mathcal{M}$, which is determined by the electric charges of the participating hadrons. Again, let us mention here that in case of collinear kinematics, the non-conserving contributions cancel for the transverse gauge of the photon polarization, as one can see from the substitution (25).

It follows, that in collinear regime, we can take the parametrizations (33) and (34), with a different form

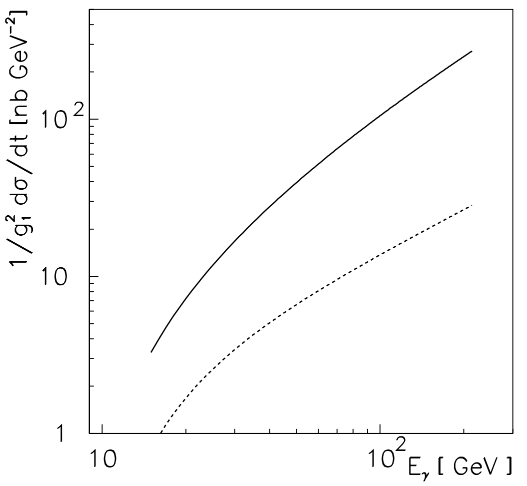

Fig. 2. Reduced differential cross-section, as a function of E_γ, for $\gamma + p \to \Lambda_c^+ + \overline{D^{*0}}$ (solid line), and $\gamma + p \to \Sigma_c^{++} + D^{*-}$ (dashed line).

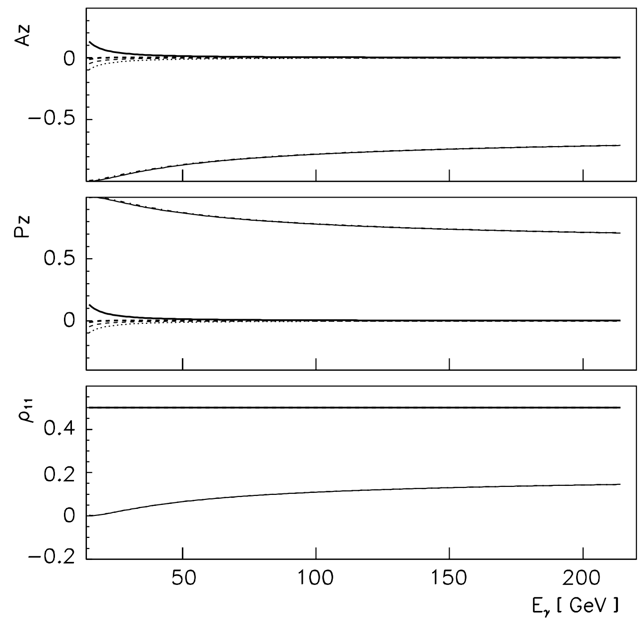

Fig. 3. Different polarization observables: asymmetry A_z (top), polarization P_z (center) and ρ_{11} (bottom), for the six considered reactions as a function of E_γ: $\gamma + p \to \Lambda_c^+ + \overline{D}^{*0}$ (solid line), $\gamma + p \to \Sigma_c^+ + \overline{D}^{*0}$ (dashed line), $\gamma + p \to \Sigma_c^{++} + D^{*-}$ (dotted line), $\gamma + n \to \Lambda_c^+ + D^{*-}$ (dash-dotted line), $\gamma + n \to \Sigma_c^+ + D^{*-}$ (thick solid line), $\gamma + n \to \Sigma_c^0 + \overline{D^{*0}}$ (thick dashed line).

factor for each diagram and with independent values of the cut-off parameters, without violation of the gauge invariance.

5 Discussion of numerical predictions

Using the expressions for the collinear amplitudes f_i, $i = 1$–3, (see appendix) and the numerical values for the strong and electromagnetic couplings given above, we can predict the E_γ-behavior of the differential cross-section, $\mathrm{d}\sigma/\mathrm{d}t$ and of some polarization observables for the collinear regime. We will consider, more exactly, only forward production. In this kinematics, the contributions of baryonic exchanges are negligible, rapidly decreasing with energy, in comparison with t-channel contributions due, on one side, to the effect of the two form factors, $F_N(s)$ and $F_Y(u)$, and, on another side, to the relative size of the t, s, and u propagators. Therefore, in the numerical estimations, the t-channel contribution dominates. Assuming, for simplicity, a common form factor for the $D + D^*$ contributions:

$$F(t) = \left(\frac{\Lambda^2 - m_D^2}{\Lambda^2 - t}\right)^2,$$

corresponding to $\Lambda_1 = \Lambda_2 = \Lambda$, we take Λ as a free parameter, to be adjusted on the data.

For an exponential t-dependence of the cross-section, for $\gamma + N \to Y_c + \overline{D}^*$ processes:

$$\frac{\mathrm{d}\sigma}{\mathrm{d}t} = \left(\frac{\mathrm{d}\sigma}{\mathrm{d}t}\right)_{\theta=0} e^{b(t-t_{\max})},$$

with $t_{\max} = m_v^2 - 2|\mathbf{k}|(E_v - |\mathbf{q}|)$ ($\mathbf{q}$ is the three-momentum of the produced $\overline{D}^*$), one can find for the total cross-section:

$$\sigma(\gamma N \to Y_c D^*) = \frac{1}{b}\left(\frac{\mathrm{d}\sigma}{\mathrm{d}t}\right)_{\theta=0}.$$

Without direct experimental information about the cross-section for the processes $\gamma + N \to Y_c + \overline{D}^*$, we take a conservative assumption:

$$\sigma\left(\gamma N \to Y_c\overline{D}^*\right) \simeq 0.1\sigma_T(\gamma N \to \text{open charm}),$$

in the interval $E_\gamma = 100$–$200\,\mathrm{GeV}$. For $b \simeq 5\,\mathrm{GeV}^{-2}$, according to the analysis [11], we find that

$$\left(\frac{\mathrm{d}\sigma}{\mathrm{d}t}\right)_{\theta=0} \simeq b\sigma_T(\gamma N \to \text{open charm}) \simeq 250\ \mu\mathrm{b\,GeV}^{-2}, \tag{35}$$

at $E_\gamma = 200\,\mathrm{GeV}$. Then, we fix $\Lambda \simeq 2.5\,\mathrm{GeV}$, in agreement with the value previously used for the calculation of associative charm production, $N + N \to N + Y_c + \overline{D}$, near threshold [23,24]. The differential cross-section, $\mathrm{d}\sigma/\mathrm{d}t$ (more exactly, the reduced differential cross-section, $1/g_1^2\ \mathrm{d}\sigma/\mathrm{d}t$) is shown as a function of E_γ, in fig. 2, for two reactions, $\gamma + p \to \Lambda_c^+ + \overline{D}^{*0}$ (solid line) and $\gamma + p \to \Sigma_c^{++} + D^{*-}$ (dashed line). Note that the reduced cross-section does not depend on the constant g_1, which is different for the different reactions. Therefore, we report the results for two reactions, only.

One can see that, in the considered model, the Λ_c production has the largest reduced cross-section. The fact that all four reactions, $\gamma + N \to \Sigma_c + \overline{D}$, are one order of magnitude smaller, is due to the difference between the values of $r_{12}(Y)$ for the $N \to \Lambda_c\overline{D}^*$ and $N \to \Sigma_c\overline{D}^*$ vertices: the "magnetic" combination $g_1 + g_2$ of the corresponding coupling constants cancels for $r_{12}(\Sigma) = -1$. This is also the reason of the difference of the polarization observables for Λ_c and Σ_c photoproduction (fig. 3).

Note that all polarization observables do not depend on the form factor $F(t)$ and on the coupling constant g_1.

However, the absolute values of the cross-section for any process $\gamma+N\to Y_c+\overline{D}^*$, calculated with the coupling constants g_1, eq. (32), are too large, in comparison with the expectation (35). This means that $SU(4)$ symmetry is strongly violated, with respect to these constants, in agreement with a previous observation [4].

The density matrix element is almost independent of energy (fig. 3c), and $\rho_{11}\simeq 0.5$ for $\gamma+N\to\Lambda_c+\overline{D}^*$, whereas $\rho_{11}\le 0.2$ for $\gamma+N\to\Sigma_c+\overline{D}^*$. The maximal value of ρ_{11} produces a $\sin^2\theta$-distribution of the produced D-meson, through the decay $D^*\to D+\pi$ (θ is the angle between the $\mathbf{k}$-direction and the direction of the D-meson three-momentum in the D^* rest system). Such θ-dependence results in a depletion of D-meson production at small angles, which should be observed, for example, in the COMPASS experiment.

The large (in magnitude) and negative values of the asymmetry A_z, for $\boldsymbol{\gamma}+\mathbf{N}\to\Lambda_c^+ + \overline{D}^*$, are near the limiting value $A_z=-1$; more exactly, $|A_z|\ge 0.8$, for $E_\gamma\le 100\,\mathrm{GeV}$.

If one considers this reaction as a background for the PGF mechanism, one can estimate the effect of this result on the extraction of ΔG. The PGF asymmetry, A_{PGF}, is predicted by perturbative QCD, on the basis of the hard subprocess $\boldsymbol{\gamma}+G\to c+\overline{c}$ [3], and can be related to the gluon contribution to the nucleon spin. The contribution of the exclusive process $\boldsymbol{\gamma}+\mathbf{N}\to Y_c+\overline{D}^*$ to the asymmetry, can be parametrized as follows:

$$A(\boldsymbol{\gamma}\mathbf{N}\to\mathrm{charm}+X)=\frac{A_{\mathrm{PGF}}+RA_z\big(\boldsymbol{\gamma}N\to Y_c\overline{D}^*\big)}{1+R}, \quad (36)$$

where $R=\sigma(\gamma N\to Y_c\overline{D}^*)/\sigma(\gamma N\to \mathrm{charm}+X)$, neglecting, for simplicity, other sources of background due to additional channels of charm particle photoproduction. In case of $R\ll 1$, we can write

$$A(\boldsymbol{\gamma}\mathbf{N}\to\mathrm{charm}+X)=A_{\mathrm{PGF}}+\Delta A,$$
$$\Delta A=R\big[A_z\big(\boldsymbol{\gamma}N\to Y_c\overline{D}^*\big)-A_{\mathrm{PGF}}\big]. \quad (37)$$

One can see that in case of opposite signs of the two asymmetries, the "dilution factor", $1/(1+R)$ and the background A_z-contribution, due to the channel $\boldsymbol{\gamma}+N\to Y_c+\overline{D}^*$, act coherently in increasing the correction ΔA (in absolute value). For example, if $R\simeq 0.1$, $A_{\mathrm{PGF}}\simeq 0.3$ and $A_z(\boldsymbol{\gamma}N\to Y_c\overline{D}^*)\simeq -1$, one can find $\Delta A\simeq -0.13$, which represents a correction $\delta A/A_{\mathrm{PGF}}\simeq 43\%$. This is a large correction, even for a relatively small contribution of the considered exclusive channel to the total cross-section.

The energy behavior of the collinear amplitudes, f_1, f_2 and f_3E_v/m_v, for the different channels $\gamma+N\to Y_c\overline{D}^*$, is shown in fig. 4, taking into account the form factors for the $s+u+t$ contributions. Due to the fact that the baryonic contributions are small, the relative values of these amplitudes are independent of the form factor. The specific factor, E_v/m_v, which has been introduced for the amplitude f_3, results from the relativistic description of the D^*-meson polarization properties. The collinear amplitude f_3 describes the D^* production with longitudinal polarization, $\mathbf{U}\cdot\hat{\mathbf{k}}\neq 0$, and the z-component of such polarization has to be equal to E_v/m_v, due to the orthogonality condition, $U\cdot q=0$.

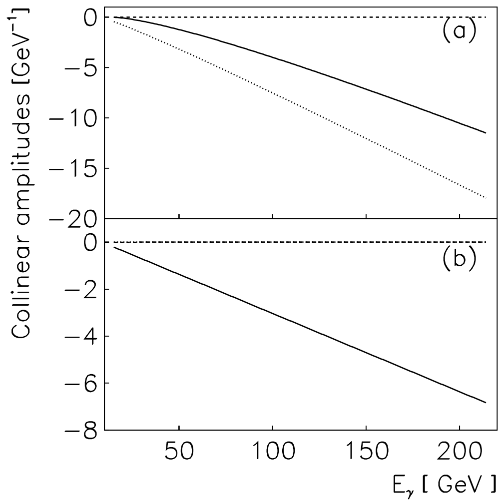

Fig. 4. Collinear amplitudes f_1 (solid line), f_2 (dashed line), and f_3E_v/m_v (dotted line), as functions of E_γ for $\gamma+p\to\Lambda_c^+ + \overline{D^{*0}}$ (a) and $\gamma+p\to\Sigma_c^{++}+D^{*-}$ (b).

Note that the different contributions, taken into account in the present model, have very simple and transparent polarization properties, especially in collinear kinematics. For example, the pseudoscalar $\overline{D}$-exchange, which induces a single collinear amplitude, f_2, results in the following values of the polarization observables:

$$\rho_{11}=1/2,\ A_z=P_z=0,\ D_{zz}=1,\ D_{xx}=D_{yy}=0. \quad (38)$$

These numbers reflect the fact that a zero-spin exchange does not transfer any information on the polarization from the electromagnetic to the strong vertex. The D^*-vector exchange, which is characterized by a non-zero anomalous magnetic moment $\kappa(D^*)$, results in $f_2=0$. This means that the $D\otimes D^*$-interference vanishes for $\mathrm{d}\sigma/\mathrm{d}t$ and ρ_{11}. Note that $A_z=-P_z$ for D^*-exchange only, independently of the photon energy E_γ. Therefore, the inequality $A_z+P_z\neq 0$ characterizes the size of the $D\otimes D^*$-interference, being sensitive to the sign of the ratio $r(Y)$.

The N-exchange in s-channel gives $f_1=f_2$, which results in $A_z=-1$, independently of the reaction channel, photon energy and numerical values of the coupling constants. This result follows from the helicity properties of the s-channel, where the spin 1/2 in the intermediate state forbids the helicity transition $\pm 3/2\to\pm 3/2$, which is characterized by the combination of collinear amplitudes f_1-f_2. But ρ_{11} and P_z can take any value in the allowed limits:

$$0\le\rho_{11}\le 1/2,\qquad 0\le|P_z|\le 1.$$

Finally, for the u-channel contribution (with $f_1 = -f_2$), the discussed polarization observables can take any value, but $P_z = -1$, for all reactions and at any photon energy.

Polarization phenomena depend strongly on the relative role of these contributions and may show large sensitivity to the value of the strong and electromagnetic coupling constants.

6 Conclusions

We considered the exclusive photoproduction of charmed vector mesons, $\gamma + N \to Y_c + \overline{D}^*$, in collinear kinematics, where the differential cross-section is large and the spin structure of the matrix element is essentially simplified. We analyzed firstly the single- and double-spin polarization phenomena, in a general form, in terms of three independent collinear amplitudes. The energy dependence of these amplitudes has been predicted —for the six possible processes— in a QCD-inspired model, which is the basis of an effective Lagrangian approach. The strong-coupling constants for the vertices $N \to Y_c + \overline{D}$ and $N \to Y_c + \overline{D}^*$ can be related through $SU(4)$ symmetry with the corresponding coupling constants for strange particles, *i.e.* for the vertices $N \to Y + K$ and $N \to Y + K^*$, $Y = \Lambda$ or Σ-hyperon, which are known from the analysis of experimental data concerning photo- and electroproduction of strange particles.

The electromagnetic characteristics of charmed particles, such as the magnetic moments of the charmed Y_c-hyperons and the transition magnetic moments for the decays $D^* \to D + \gamma$, have been estimated in the framework of the quark model.

As the baryonic exchanges (by N in the s-channel and Y_c in the u-channel) are negligible in the considered model, the polarization observables are quite insensitive to this form factor, and to the vector coupling constant $g_1(NY_c\overline{D}^*)$ as well. Therefore, this model gives robust predictions for the polarization effects. The large and negative values of the asymmetry A_z (for the collision of a circularly polarized photon beam with a longitudinally polarized nucleon target) for Λ_c^+ production on proton and neutron targets (which is a factor ten larger in comparison with Σ_c production) can be a source of large systematic error in the extraction of ΔG from $\boldsymbol{\gamma} + \mathbf{N} \to \text{charm} + X$, even in case of a relatively small cross-section of the considered exclusive reactions.

A reasonable value for the cross-section of the considered processes can be obtained only for a smaller value of the coupling constants $g_1(NY_cD^*)$, in comparison with $SU(4)$ predictions.

We thank the members of the Saclay group of the COMPASS collaboration, for interesting discussions and useful comments.

Appendix A

Here we give the expressions for the scalar amplitudes f_i, $i = 1$–3:

$$f_i = f_{i,t}(D) + f_{i,t}(D^*) + f_{i,s} + f_{i,u} \, ,$$

where the indices s, u, and t correspond to s-, u-, and t-channel contributions.

– t-channel (D contribution):

$$f_{1,t}(D) = f_{3,t}(D) = 0,$$

$$f_{2,t}(D) = \kappa\left(D^{*0}\overline{D}\gamma\right)\frac{g(Y_c)}{2m_v}\frac{t-m_v^2}{t-m_D^2}\left(1-Q-\frac{2m}{W+m}\right);$$

– t-channel (D^* contribution):

$$f_{1,t}(D^*) = \frac{\kappa(D^*)}{2}\left(\frac{m-M}{m_v^2}+\frac{r_{12}}{m+M}\right)$$
$$+\kappa(D^*)WR_D\left[(1+r_{12})(1+Q)-r_{12}\frac{W+m}{M+m}\right],$$

$$f_{2,t}(D^*) = 0,$$

$$f_{3,t}(D^*) = -\frac{\kappa(D^*)}{2}(1+r_{12})$$
$$\times R_D\left[W-m+(W+m)Q\right],$$

with $R_D = \frac{E_v+q}{m_v^2(W-m)}$;

– s-channel:

$$f_{1,s} = f_{2,s} = \frac{e(N)}{W+m}(1+Q)+\frac{\kappa(N)}{2m}$$
$$\times\left(Q-1+\frac{2m}{W-m}\right)-\frac{e(N)}{W+m}\frac{r_{12}}{m+M}$$
$$\times\left[(W-m)-Q(W+m)\right]+\frac{\kappa(N)}{2m}\frac{r_{12}}{m+M}$$
$$\times\left[(W-m)\left(1+\frac{2m}{W+m}\right)+Q(W+m)\right],$$

$$f_{3,s} = \frac{e(N)}{W+m}(-1+Q)\left(1-\frac{q}{q_0}\right)$$
$$+\frac{\kappa(N)}{2m}\left\{Q+1-\frac{2m}{W-m}\right.$$
$$\left.+\left[1+\left(1-\frac{2m}{W+m}\right)Q\right]\frac{q}{q_0}\right\}$$
$$+\frac{e(N)}{W+m}\frac{r_{12}}{m+M}\left(1-\frac{q}{q_0}\right)$$
$$\times\left[(W-m)+Q(W+m)\right]+\frac{\kappa(N)}{2m}\frac{r_{12}}{m+M}$$
$$-\left\{(W+m)Q-(W-M)\left(1-\frac{2m}{W+m}\right)\right.$$
$$\left.\times\left[W-m-Q(W+m)\left(1-\frac{2m}{W+m}\right)\right]\frac{q}{q_0}\right\}.$$

– u-channel:

$$f_{1,u}=f_{2,u}=R_u\left\{e(Y)+\frac{\kappa(Y)}{2M}\left[M-(q+E_2)\frac{m}{W}\right]\right.$$
$$+e(Y)\frac{r_{12}}{m+M}(q_0-q)\frac{m}{W}$$
$$+\frac{\kappa(Y)r_{12}}{M(m+M)}(q_0+q)$$
$$\left.\times\left[-q-E_2+m\frac{m}{W}\left(\frac{q_0-q}{q_0+q}\right)\right]\right\}$$
$$f_{3,u}=R_u\left\{e(Y)\frac{m}{W}\left(1-\frac{q}{q_0}\right)\frac{\kappa(Y)}{2m}\left[-(q+E_2)\left(1+\frac{q}{q_0}\right)\right.\right.$$
$$\left.+m\frac{M}{W}\left(1-\frac{q}{q_0}\right)\right]+e(Y)\frac{r_{12}}{m+M}\frac{m_v^2}{q_0}$$
$$+\frac{\kappa(Yr_{12})}{M(m+M)}(q+q_0)\left[M-(q+E_2)\frac{m}{W}\left(\frac{q_0-q}{q_0+q}\right)\right.$$
$$\left.\left.-\left(M+(q+E_2)\frac{m}{W}\left(\frac{q_0-q}{q_0+q}\right)\right)\frac{q}{q_0}\right]\right\}$$

with $R_u=(1+Q)\frac{W(E_2-q)}{M^2(W+m)}$, $Q=\frac{q}{E_2+M}$, $E_2=\frac{s+M^2-m_v^2}{2w}$, and $q_0=W-E_2$.

References

1. E. Tomasi-Gustafsson, M.P. Rekalo, Phys. Rev. D **69**, 094015 (2004).
2. G.K. Mallot, J. Phys. G **25**, 1539 (1999); M. Ryskin, E. Leader, J. Phys. G **25**, 1541 (1999).
3. L.M. Jones, H.W. Wyld, Phys. Rev. D **17**, 759 (1978); F. Halzen, D.M. Scott, Phys. Lett. B **72**, 404 (1978); H. Fritzsch, K.H. Streng, Phys. Lett. B **72**, 385 (1978); V.A. Novikov, M.A. Shifman, A.I. Vainstein, V.I. Zakharov, Nucl. Phys. B **136**, 125 (1978) (Yad. Fiz. **27**, 771 (1978)); J. Babcock, D.W. Sivers, S. Wolfram, Phys. Rev. D **18**, 162 (1978).
4. M.P. Rekalo, E. Tomasi-Gustafsson, Phys. Rev. D **65**, 074023 (2002) and references herein.
5. COMPASS Collaboration (G. Baum *et al.*), CERN-SPSLC-96-14.
6. ZEUS Collaboration (M. Derrick *et al.*), Phys. Lett. B **349**, 225 (1995); H1 Collaboration (S. Aid *et al.*), Nucl. Phys. B **472**, 32 (1996).
7. SLAC Hybrid Facility Photon Collaboration (K. Abe *et al.*), Phys. Rev. D **33**, 1 (1986).
8. Photon Emulsion Collaboration (M.I. Adamovich *et al.*), Phys. Lett. B **187**, 437 (1987).
9. NA14/2 Collaboration (M.P. Alvarez *et al.*), Z. Phys. C **60**, 53 (1993).
10. Tagged Photon Spectrometer Collaboration (J.C. Anjos *et al.*), Phys. Rev. Lett. **62**, 513 (1989).
11. K. Sliwa *et al.*, Phys. Rev. D **32**, 1053 (1985).
12. FOCUS Collaboration (J.M. Link *et al.*), Phys. Lett. B **566**, 51 (2003).
13. T.M. Aliev, E. Iltan, N.K. Pak, M.P. Rekalo, Z. Phys. C **64**, 683 (1994).
14. H. Rubinstein, L. Stodolsky, Phys. Lett. B **76**, 479 (1978).
15. SLAC Hybrid Facility Photon Collaboration (K. Abe *et al.*), Phys. Rev. D **30**, 694 (1984).
16. K. Hagiwara *et al.*, Phys. Rev. D **66**, 010001 (2002).
17. M.P. Rekalo, Ukr. Fiz. J. **22**, 1602 (1977).
18. S.K. Bose, L.P. Singh, Phys. Rev. D **22**, 773 (1980).
19. S.N. Jena, D.P. Rath, Phys. Rev. D **34**, 196 (1986).
20. M.J. Savage, Phys. Lett. B **326**, 303 (1994).
21. V.M. Samsonov, Nucl. Instrum. Methods B **119**, 271 (1996).
22. M. Guidal, J.M. Laget, M. Vanderhagen, Nucl. Phys. A **627**, 645 (1997).
23. M.P. Rekalo, E. Tomasi-Gustafsson, Phys. Rev. C **67**, 044004 (2003) and references herein.
24. A.M. Gasparyan, V.Y. Grishina, L.A. Kondratyuk, W. Cassing, J. Speth, arXiv:nucl-th/0210018.